

Short communication

# Liquid permeation through cast tape of graphite particles based on non-uniform packing structure

Boris Golman<sup>a,\*</sup>, Keisuke Seino<sup>a</sup>, Kunio Shinohara<sup>a</sup>, Katsutomo Ohzeki<sup>b</sup>

<sup>a</sup> *Division of Chemical Process Engineering, Graduate School of Engineering, Hokkaido University, West 8, North 13, Kita-Ku, Sapporo, Hokkaido 060-8628, Japan*

<sup>b</sup> *Fine Materials and Components Division, Hitachi Powdered Metals Co., Ltd., 1 Mito, Tako-machi, Katori-gun, Chiba 289-2247, Japan*

Available online 30 May 2006

## Abstract

In the present study, the rate of liquid permeation is measured for green and pressed tapes used as an anode film of lithium ion battery. The tape was made of graphite particles of various shapes which were modified by high-speed rotational blending. The packing structure was measured by image analysis on the cross-sections of the tape in three dimensions and was characterized by a distribution of void sizes among particles. Based on the void size distribution, the mathematical model of permeation was developed considering the tape porous structure as the bundle of parallel pipes of various sizes.

As a result, the liquid permeation data with the graphite tapes can successfully be described with the developed model, in contrast with much higher permeation rate by Kozeny–Carman's equation. The permeation rate was also confirmed to get higher for the tape made of spherical particles as a result of higher equivalent diameter due to wider void size distribution and lower tortuosity owing to more regular packing structure.

© 2006 Elsevier B.V. All rights reserved.

*Keywords:* Natural graphite; Particle shape modification; Cast tape; Liquid permeation; Tape microstructure; Lithium ion battery

## 1. Introduction

Modern consumer and industrial electronic devices require lithium ion batteries of large capacity with high charge–discharge capability. Such batteries utilize tape casts of graphite particles as a negative electrode. Ohzeki et al. [1] confirmed that the porous structure of the tape significantly influences on battery characteristics. Expansion of graphite crystals during charging owing to the intercalation of Li ions and subsequent constriction during discharge result in the liquid movement in and out of the tape. To estimate the degree of this phenomenon, liquid permeation through void spaces among packed graphite particles inside the tape is investigated in the present research. Then, the enhancement of liquid permeation should be useful for improving battery performances at high rate [2].

The void structure formed during casting and pressing of highly non-regular shape graphite particles is very complex [3]. Models utilizing Kozeny–Carman's equation could not successfully relate the permeation rate to the structure of porous medium due to its oversimplified representation of packing structure with an effective hydraulic diameter.

The objective of the present research is to investigate experimentally and theoretically the relationship between the liquid permeation rate and porous structure of tapes cast with graphite particles of various shapes which are modified by high-speed rotational blending.

## 2. Theoretical

### 2.1. Tape microstructure

In the present study, the structure of void space inside the packed bed of particles forming the tape is supposed to be represented as a bundle of parallel but bended tubes of various diameters. Tape microstructure was characterized by the distribution of void sizes among packed particles [4]. The distribution

\* Corresponding author. Tel.: +81 11 706 6592; fax: +81 11 706 6593.  
E-mail address: [golman@eng.hokudai.ac.jp](mailto:golman@eng.hokudai.ac.jp) (B. Golman).

of the probability,  $P_2$ , of finding circular void of a given size,  $\chi_2$ , in the packing of non-spherical particles was derived on the basis of the model of spherical particles [5] as follows:

$$P_2(\chi_2) = 3\beta \frac{\nu(1-\nu)}{1-(\nu/\nu_m)} \int_{\chi_2}^{\infty} (1+\beta\chi_3)^2 \sqrt{1-\left(\frac{\chi_2}{\chi_3}\right)^2} \times \exp\left\{-\frac{\nu}{1-(\nu/\nu_m)}[(1+\beta\chi_3)^3-1]\right\} d\chi_3 \quad (1)$$

where  $\nu$  is the packing density,  $\nu_m$  the limiting packing density,  $\beta$  the shape coefficient relevant to the particle packing and  $\chi_3$  is the diameter of the spherical void normalized by the associated average particle size, respectively. The particle size distribution was measured on the volume basis and  $\beta$  was assumed to be equal to one in the present research. Then, the void size distribution measured by image analysis was successfully fitted to Eq. (1) with  $\nu_m$  as a fitting parameter.

### 2.2. Liquid permeation through tape

The mean velocity,  $u_{e,i}$ , of streamline liquid flow through the tube of diameter,  $d_{t,i}$ , is given by a Hagen–Poiseuille law as:

$$u_{e,i} = \frac{\Delta p d_{t,i}^2}{32 L_{e,i} \mu} \quad (2)$$

where  $\Delta p$  is the pressure drop,  $L_{e,i}$  the tube length and  $\mu$  is the liquid viscosity. Then, the superficial velocity of liquid flowing through the bed of particles of thickness,  $L_b$ , and the total cross-sectional area,  $A_b$ , is given as:

$$u_{b,0} = \frac{\pi}{4 A_b} \sum_{i=1}^m n_i d_{t,i}^2 \langle u_{e,i} \rangle \quad (3)$$

Here,  $n_i$  is the number of tubes of diameter  $d_{t,i}$  and  $m$  is the total number of tube diameters. Introducing Eq. (2) into Eq. (3) we can obtain the following equation:

$$u_{b,0} = \frac{\pi \Delta p}{128 A_b \mu} \sum_{i=1}^m \frac{n_i d_{t,i}^4}{L_{e,i}} \quad (4)$$

Here, we assume that the distribution of tube diameters,  $f_i$ , can be expressed as the distribution of the void sizes among the particles [6]:

$$f_i \Delta d_{v,i} = P_i - P_{i+1} \quad (5)$$

Then, the number of tubes is as follows:

$$n_i = A_b \varepsilon \frac{f_i \Delta d_{v,i}}{\sum ((\pi/4) d_{v,i}^2 f_i \Delta d_{v,i})} \quad (6)$$

Using Eq. (6) and assuming that tubes are of equal length  $L_e$ , pressure drop  $\Delta p$  can be deduced as:

$$\frac{\Delta p}{L_b} = 32 \left( \frac{L_e}{L_b} \right) \frac{\mu u_{b,0}}{\varepsilon} \left( \sum_{i=1}^m \frac{f_i \Delta d_{v,i} d_{v,i}^4}{\sum (d_{v,i}^2 f_i \Delta d_{v,i})} \right)^{-1} \quad (7)$$

Here, the equivalent diameter,  $D_e$ , can be defined as:

$$D_e = \sqrt{\frac{\sum_{i=1}^m f_i \Delta d_{v,i} d_{v,i}^4}{\sum (d_{v,i}^2 f_i \Delta d_{v,i})}} \quad (8)$$

## 3. Experimental

### 3.1. Particle shape modification

Natural graphite particles of median diameter,  $d_p = 45.0 \mu\text{m}$ , and of flaky shape were used as a raw material as supplied by Hitachi Powdered Metals Co. The particle size was measured by a laser diffraction method (PRO-7000, Seishin Kogyo Co.). The particle shape was modified with high-speed rotational blending machine (Hybridization System, Nara Machinery Co.) by varying peripheral velocity and treatment time [7]. The particle shape was characterized by a shape index,  $K$ , as a ratio of short to long axis of an approximate ellipse [8]. An ellipse was constructed on the basis of Fourier analysis of particle outline detected by image analysis on binarized SEM photographs. Indices averaged for at least 30 particle outlines were reported here as  $K_{av}$ . The SEM photographs of particles used for tape casting are shown in Fig. 1.

### 3.2. Tape casting and morphology of porous microstructure

Tape casting was performed on a laboratory casting machine (PI-1210, Tester Sangyo Co.) with a blade with a gap of  $200 \mu\text{m}$  moving at constant speed over the slurry, which was prepared by mixing particles with binders, styrene-butadiene rubber emulsion and carboxyl methyl cellulose, in distilled water. Green tapes thus obtained were dried at  $393 \text{K}$  for 10 min. Green tapes were pressed with a roller press to yield pressed tapes of constant thickness of  $70 \mu\text{m}$  and bulk density of  $1.5 \text{g cm}^{-3}$ .

The tape cross-sections were observed by SEM in three different directions on tape samples mounted into resin separately for each surfaces. Here, the tape surface parallel to the casting direction is denoted as  $X$  surface, while  $Y$  surface is perpendicular to the cast one and  $Z$  is the top surface. The distribution of void sizes among packed particles in the cross-section was measured by randomly placing void circles of various sizes all over the binary image as described in detail elsewhere [6].

### 3.3. Measurements of liquid permeation

Liquid permeation through the tape was measured with a device manufactured by Jacom Co., as shown in Fig. 2. Liquid was supplied to the cell at desired flow rate by a custom-made syringe pump. The pressure difference was measured with a pressure gauge during flow in  $Z$  direction across the tape fixed inside the permeation cell. In the beginning of the experiment air trapped inside the tape was removed with vacuum pump and liquid was filled inside the cell.

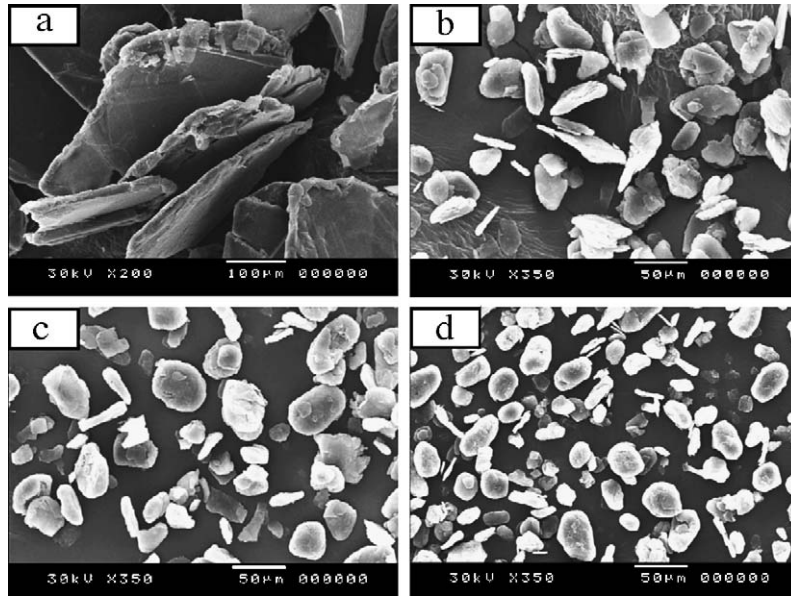


Fig. 1. SEM photos of (a) raw and modified particles (b)  $K_{av} = 0.628$ , (c)  $K_{av} = 0.657$ , (d)  $K_{av} = 0.741$ .

4. Results and discussions

4.1. Porous microstructure of tape

The distributions of void sizes measured separately on X, Y and Z surfaces of the pressed tape are shown in Fig. 3. The distribution over Z surface is wider than those over X and Y surfaces, confirming the existence of non-spherical shape voids with longer axis on Z surface. The distributions are wider for tapes cast with more spherical particles, as exemplified by higher value of the limiting packing density  $v_m$ . The arrangement of non-spherical particles with longer side aligned with cast direction during casting and pressing results in elimination of large voids. On the other hand, particles of rounder shape are arranged in such a way that they can keep the void shape and size against press. As a result, the larger voids still exist in such tapes.

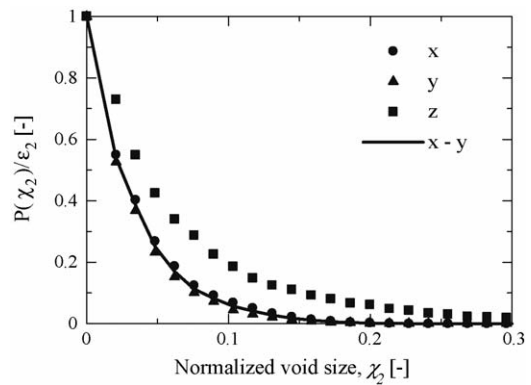


Fig. 3. Void size distributions of pressed tape.

4.2. Liquid permeation

The change in the pressure drop across the tape with liquid flow rate is shown in Fig. 4. Experimental data are well fitted with line, calculated by Eq. (7) with equivalent diameter defined by

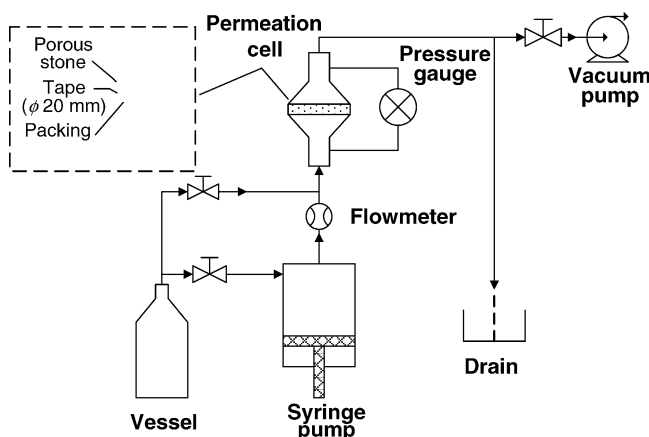


Fig. 2. Experimental setup for liquid permeation measurement.

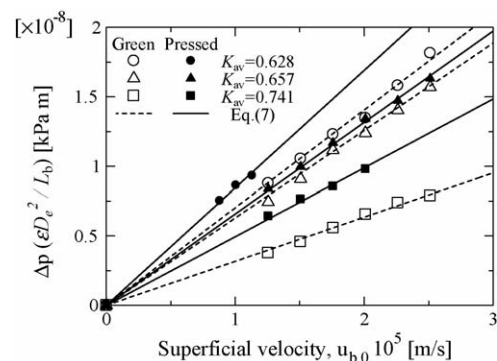


Fig. 4. Variation of pressure drop across tape with liquid flow rate.

Eq. (8) using void size distribution, confirming the applicability of the above model of permeation. The pressure drop decreases for the tape cast with particles of more spherical shape owing to existence of large voids.

We also tried to fit experimental data with Kozeny–Carman's model which frequently used for correlating pressure drop with mean velocity for flow through a packed bed. The model by Eq. (9) adopts the concept of an effective hydraulic diameter to express the effect of the bed structure on the flow as:

$$\frac{\Delta p}{L_b} = \frac{5(1 - \varepsilon)^2 S_V^2 \mu u_{b,0}}{\varepsilon} \quad (9)$$

where  $S_V$  is the specific surface area on the basis of net particle volume. However, the pressure drop calculated by Eq. (9) is 100 times lower than the measured one. This difference can be explained by significantly more non-uniform structure of tape porous space formed during casting and pressing in comparison with that for a packed bed.

The distributions in  $X$  and  $Y$  directions are quite similar, so we combine them into one by calculating the probability of finding circular void of a given size  $P_{X-Y}$  as  $\sqrt{P_X P_Y}$ , as shown by the line in Fig. 3. It can be expected that the liquid permeation through the tape is limited by the constrictions to flow in  $X$  and  $Y$  directions inside tape porous space. The slopes of curves in Fig. 4 are proportional to so-called tortuosity of imaginary tubes,  $\tau = (L_e/L_b)$ , used to carry out liquid inside tape packing structure. The tortuosity was an adjustable parameter of our permeation model. Then, the tortuosity was correlated with characteristics of porous structure such as  $\varepsilon$  and  $v_m$  by the following equation:

$$\tau = 0.118\varepsilon^{-3.48} v_m^{-4.52} \quad (10)$$

The parameters of this equation were obtained by linear fitting of data. The tortuosity decreases with increasing  $v_m$  for green and pressed tapes. The path of liquid flowing around more spherical particles inside the tape could reasonably be expected to be shorter than that in the case of flaky particles.

On the basis of the present research, it can be concluded that the modification of the shape of graphite particles toward

more spherical one is useful for improving the liquid permeation rate through electrode tape cast of such particles in an effort to design high performance batteries. With increasing shape index of particles, the equivalent diameter increases due to existence of large voids and the tortuosity decreases owing to more regular packing structure, both of which contribute to the enhancement of liquid permeation rate.

## 5. Conclusions

The rate of liquid permeation was investigated for green and pressed electrode tapes cast with graphite particles of various shapes. The mathematical model was developed by taking into account the tape packing structure characterized by the distribution of void sizes among particles as measured by image analysis on the tape cross-sections.

As a result, the liquid permeation data with the graphite tapes was successfully described with the developed model, in contrast with much higher permeation rate by Kozeny–Carman's equation. The permeation rate was confirmed to get higher for the tape made of spherical particles as a result of higher equivalent diameter due to wider void size distribution and lower tortuosity owing to more regular packing structure. Thus, the increase in the high rate discharge performance can be expected with lithium ion cells using the tape made of more spherical particles.

## References

- [1] K. Ohzeki, Y. Ohsaki, B. Golman, K. Shinohara, TANSO 213 (2004) 140.
- [2] K.K. Patel, J.M. Paulsen, J. Desilvestro, J. Power Sources 122 (2003) 144.
- [3] K. Seino, B. Golman, K. Shinohara, K. Ohzeki, TANSO 216 (2005) 2.
- [4] K. Shinohara, T. Murai, Kagaku Kogaku Ronbunshu 20 (1994) 198.
- [5] K. Alonso, E. Sainz, F.A. Lopez, K. Shinohara, Chem. Eng. Sci. 50 (1995) 1983.
- [6] B. Golman, T. Takigawa, K. Shinohara, K. Ohzeki, Colloids Surf. A Physicochem. Eng. Aspects 254 (2005) 9.
- [7] K. Ohzeki, Y. Saito, B. Golman, K. Shinohara, Carbon 43 (2005) 1673.
- [8] K. Shinohara, M. Oida, B. Golman, Powder Technol. 107 (2000) 131.